Nanosized Molecular Propellers by Cyclodehydrogenation of Polyphenylene Dendrimers

Christopher D. Simpson, Gunter Mattersteig, Kai Martin, Lileta Gherghel,
Roland E. Bauer, Hans Joachim Räder, and Klaus Müllen*

*Contribution from the Max-Planck-Institute for Polymer Research,
Ackermannweg 10, 55128 Mainz, Germany*

Received June 17, 2003; E-mail: muellen@mpip-mainz.mpg.de

Abstract: In a polymer analogous approach, large dendritic oligophenylenes containing benzene and tetraphenylmethane cores are transformed via oxidative cyclodehydrogenation to novel propeller-shaped molecules with large polycyclic aromatic hydrocarbon units as "blades". Structure analysis is performed by a combination of MALDI-TOF mass spectrometry, UV/vis, fluorescence, and Raman spectroscopy using solid-state sample preparation methods. These methods are also utilized to determine the degree of the cyclodehydrogenation reaction.

Introduction

One of the major goals of polycyclic aromatic hydrocarbon (PAH) chemistry has been the synthesis of constantly improved, molecularly defined graphite model compounds.[1−3] Significant advances toward this aim could be achieved by applying a method recently developed by us.[4,5] This approach is based on the planarization of three-dimensional, dendritic oligophenylenes, which can be drawn in their 2D-projection without overlap of any phenyl rings, by oxidative cyclodehydrogenation. It enables not only the synthesis of hexa-*peri*-hexabenzocoronene (HBC) (**4**) and its derivatives but also much larger all-benzoid PAHs with up to 222 carbons (**6**) (Scheme 1).[6] For an even larger PAH and thus improved graphite model, the 474 carbon-containing polyphenylene dendrimer **7** was a suitable precursor candidate (Scheme 2).

As it turned out in the course of this study, the geometries of the precursor molecule, and especially of its core, are of paramount importance. Not only do they influence the efficiency of the cyclodehydrogenation, but they also play an important role in the geometrical result of the planarization reaction. In fact, as described in the following, the outcome of the cyclodehydrogenation can lead to a completely different domain of chemistry than was originally intended; instead of to planar 2D-graphite model compounds, it leads to the field of three-dimensional nanostructures, such as propeller-shaped molecules,[7,8] highly nonplanar PAHs,[9] and 3D-graphitic materials.[10]

Scheme 1. Chemical Structures of the PAHs C42 (HBC) (**4**), C132 (**5**), and C222 (**6**) and Their Respective Precursor Molecules **1**, **2**, and **3**
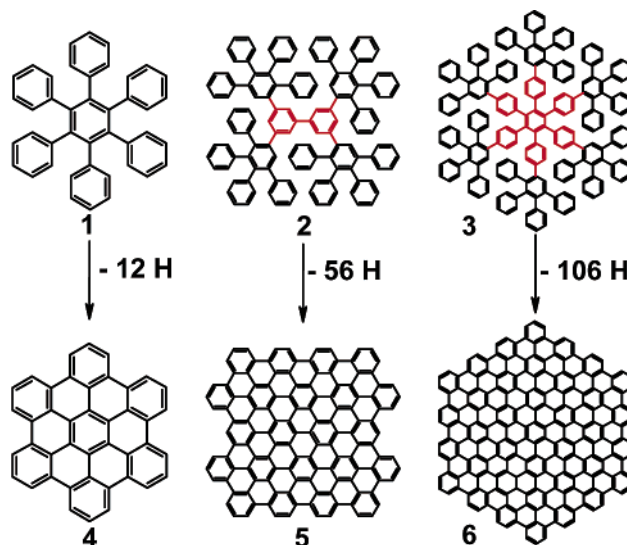

This finding prompted us to apply our cyclodehydrogenation conditions also to a dendrimer with a geometry different from that of **7**, the polyphenylene **11**. It is built around a tetrahedral core, thus separating the molecule into four dendritic arms, intentionally prohibiting total planarization (Scheme 3).

To transform the dendrimers to the corresponding target PAH structures, already 136 hydrogens for molecule **11** and 252 hydrogens for molecule **7** have to be removed in one single reaction. This sheer number sets the demands for the cyclodehydrogenation and takes it from the field of organic synthesis more into the domain of polymer analogous reactions. The increasing number of bonds to be closed results in an exponential

(1) Clar, E. *The Aromatic Sextet*; Wiley: London, 1972.
(2) Zander, M. *Polycyclische Aromaten*; Teubner: Stuttgart, 1995.
(3) Goddard, R.; Haenel, M. W.; Herndon, W. C.; Krüger, C.; Zander, M. *J. Am. Chem. Soc.* **1995**, *117*, 30−41.
(4) Watson, M. D.; Fechtenkötter, A.; Müllen, K. *Chem. Rev.* **2001**, *101*, 1267−1300.
(5) Iyer, V. S.; Wehmeier, M.; Brand, J. D.; Keegstra, M. A.; Müllen, K. *Angew. Chem., Int. Ed. Engl.* **1997**, *36*, 1604−1607.
(6) Simpson, C. D.; Brand, J. D.; Berresheim, A. J.; Przybilla, L.; Räder, H. J.; Müllen, K. *Chem.-Eur. J.* **2002**, *8*, 1424−1429.
(7) Barnett, L.; Ho, D. M.; Baldridge, K. K.; Pascal, R. A. *J. Am. Chem. Soc.* **1999**, *121*, 727−733.
(8) Vacek, J.; Michl, J. *New J. Chem.* **1997**, *21*, 1259−1268.
(9) Scott, L. T.; Boorum, M. M.; McMahon, B. J.; Hagen, S.; Mack, J.; Blank, J.; Wegner, H.; de Meijere, A. *Science* **2002**, *295*, 1500−1503.
(10) Shen, X. F.; Ho, D. M.; Pascal, R. A. *Org. Lett.* **2003**, *5*, 369−371.

Scheme 2. Chemical Structures of the Polyphenylene Dendrimer **7** ($C_{474}H_{318}$, $M = 6013$ Da), the Cyclodehydrogenation Products **8** ($C_{474}H_{66}$, $M = 5760$ Da), **9a** ($C_{474}H_{132}$, $M = 5826$ Da), and **9b** ($C_{474}H_{120}$, $M = 5814$ Da), and the Respective "Propeller Arms" **10a** ($C_{150}H_{40}$, $M = 1842$ Da) and **10b** ($C_{156}H_{40}$, $M = 1914$ Da)
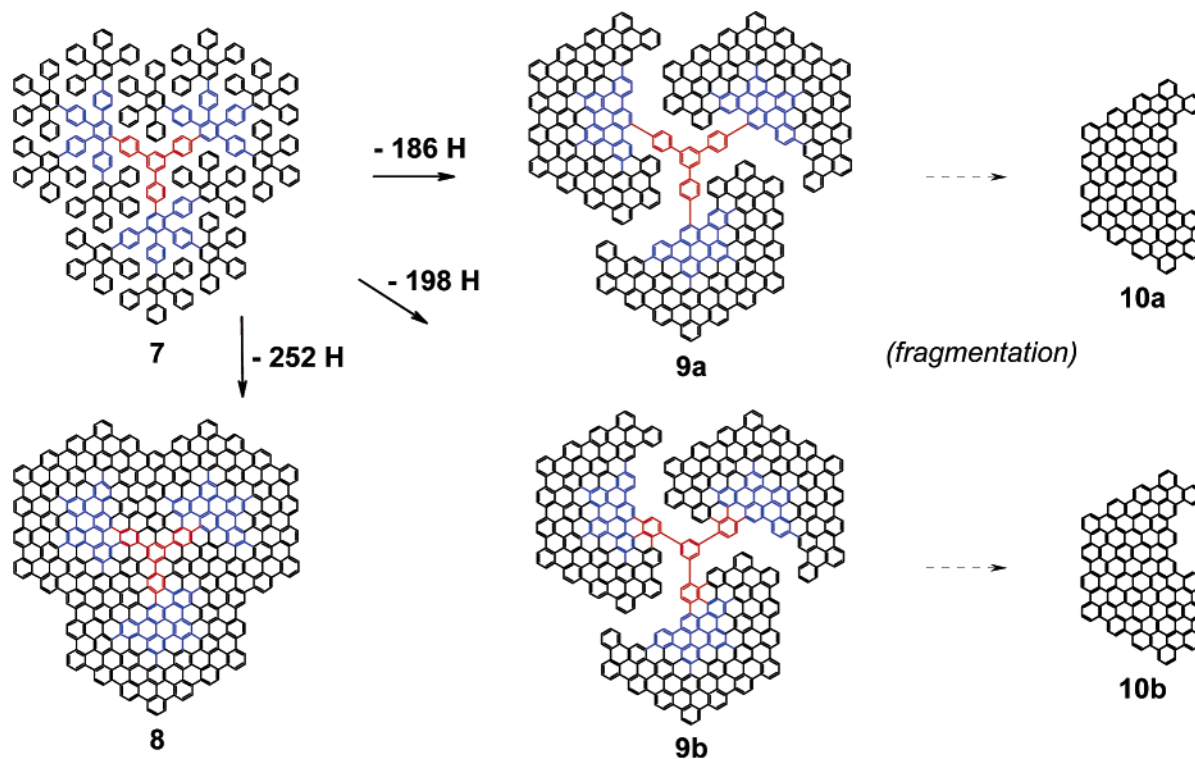
Scheme 3. Chemical Structures of the Polyphenylene Dendrimer **11** ($C_{385}H_{260}$, $M = 4886$ Da) and the Cyclodehydrogenation Products **12a** ($C_{385}H_{132}$, $M = 4757$ Da), **12b** ($C_{385}H_{128}$, $M = 4753$ Da), and **12c** ($C_{385}H_{124}$, $M = 4749$ Da)
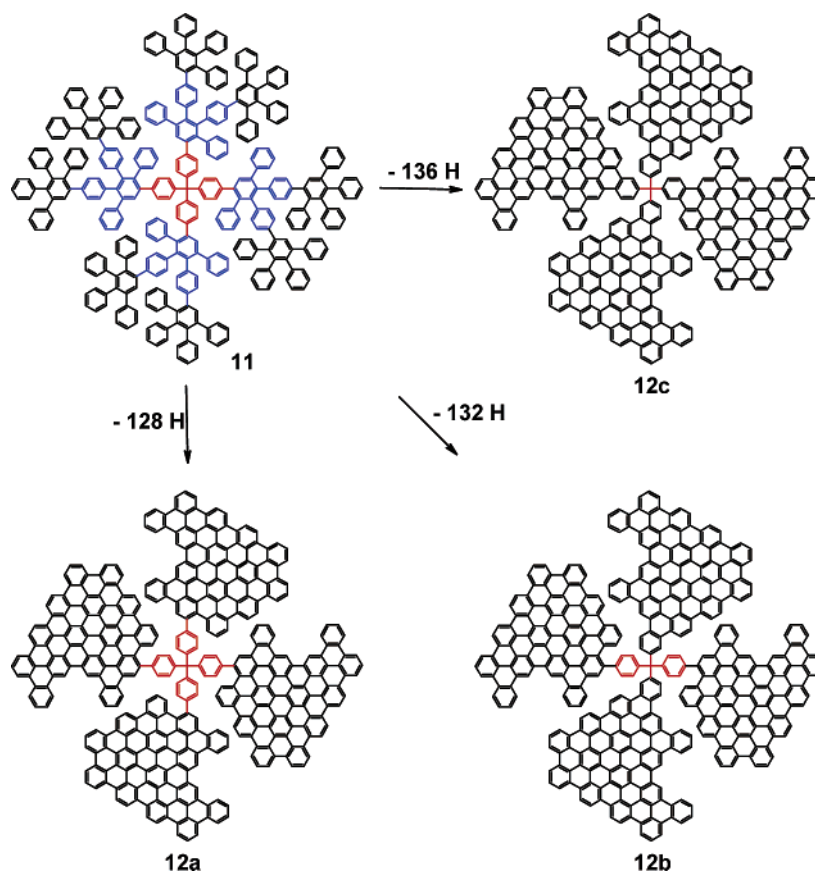
Scheme 4. Synthesis of Dendrimer **7**[a]
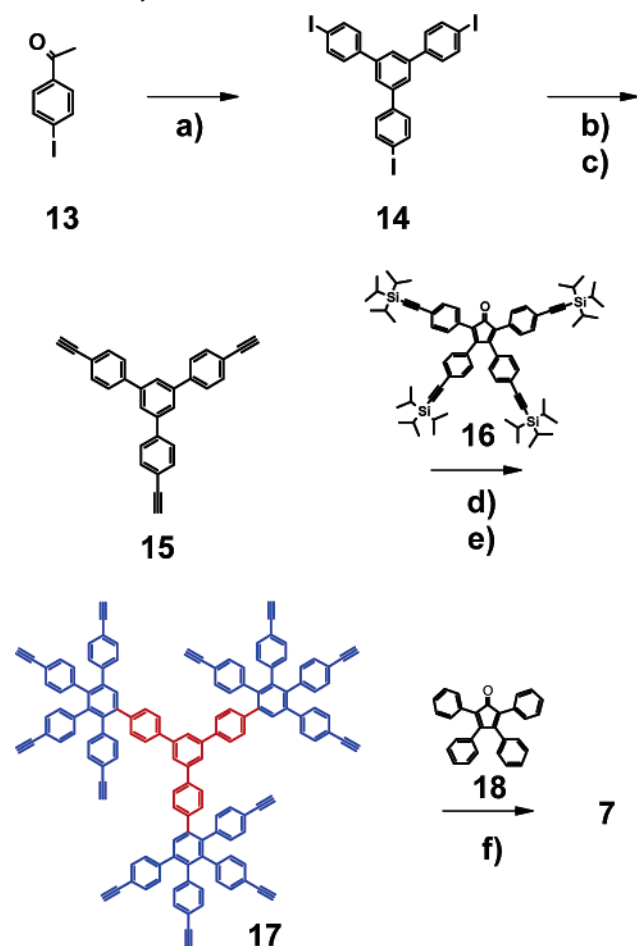
[a] Reagents, conditions, and yields: (a) SiCl$_4$, dry ethanol, 60%; (b) TMSA, CuI, Pd[PPh$_3$]$_2$Cl$_2$, PPh$_3$, NEt$_3$/THF (1:1), 97%; (c) K$_2$CO$_3$, MeOH/THF, 85%; (d) *o*-xylene, 175 °C, 14 h, 95%; (e) NH$_4$F/Bu$_4$NF, THF, 87%; (f) *o*-xylene, 175 °C, 14 h, 76%.

decrease of the overall yield. It should be considered that, for example, with the formation of 126 new bonds as for **8**, a conversion of 99% in each carbon−carbon bond formation would lead only to a total yield of 28% of desired product. To achieve at least 90% overall yield, a bond forming efficiency of 99.9% is required. This is a challenging value for any given single organic reaction, let alone for a synthesis with a multitude of individual steps which is encountered by a severe solubility problem after a few bond formations.

Results and Discussion

Dendrimer Synthesis. Dendrimer **7** is accessible in a six-step synthesis, as outlined in Scheme 4. First, 1,3,5-tris-(4-iodophenyl)-benzene (**14**) is obtained by regioselective cyclo-trimerization of 1-(4-iodophenyl)-ethanone (**13**) with silicon tetrachloride in 60% yield.[11] Through the use of iodide as a functional group, the Hagihara−Sonogashira coupling of tri-methylsilylacetylene to the core proceeds smoothly at room temperature in 97% yield.[12] The silyl protecting groups are removed under mild conditions with potassium carbonate in
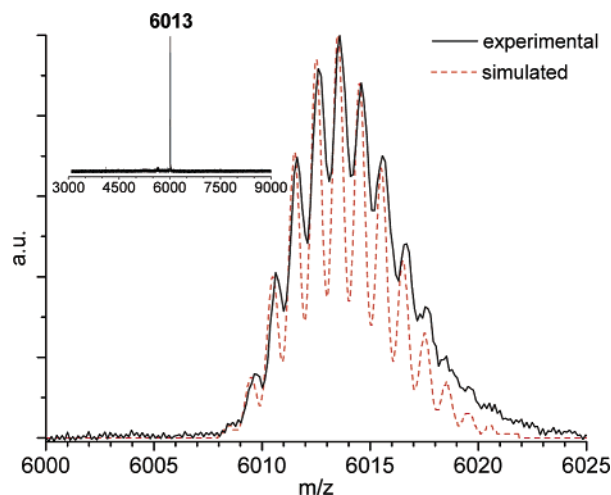
(11) Plater, M. J.; McKay, M.; Jackson, T. *J. Chem. Soc., Perkin Trans. 1* **2000**, 2695−2701.
(12) Takahashi, S.; Kuroyama, Y.; Sonogashira, K.; Hagihara, N. *Synthesis* **1980**, 627−630.

Figure 1. MALDI-TOF mass spectrum of C474-dendrimer **7**.

methanol/THF affording **15**. Diels−Alder cycloaddition of the core **15** with the cyclopentadienone **16**, a protected dendrimer branching unit, is employed under extrusion of carbon monoxide in boiling *o*-xylene to yield the protected first-generation dendrimer.[13,14] The cyclopentadienone branching units are designated by their number of reactive sites; in the case of **16**, the molecule can react with one alkyne and thereby introduces four new protected alkynes. It is therefore called an A$_4$B unit. The triisopropylsilyl protective groups of the first generation are removed with fluoride salts under more drastic conditions than for trimethylsilyl groups to obtain the deprotected first-generation dendrimer **17** in 87% yield. Finally, in a further Diels−Alder cycloaddition, **17** is reacted with tetracyclone (**18**) to yield the three-dimensional, shape-persistent[15,16] dendrimer **7** as a readily soluble and colorless compound with a molecular mass of 6013 Da, which can be completely characterized by solution NMR spectroscopy and MALDI-TOF spectrometry techniques (Figure 1).

The synthesis of the tetrahedral dendrimer **11** has been reported previously.[14] It is prepared in a way similar to **7** by reaction of A$_2$B branching units, cyclopentadienones with two protected alkynes, with a tetraphenylmethane core. After depro-tection, a further cycloaddition of tetracyclone (**18**) yields the second-generation dendrimer **11**.

Oxidative Cyclodehydrogenation and Characterization. The C474 dendrimer **7** was subjected to the typical oxidative cyclodehydrogenation conditions developed for the synthesis of large, unsubstituted PAHs.[6] After reaction with different quantities of aluminum(III) chloride and copper triflate in carbon disulfide, mass spectrometry suggested chlorination and incom-plete dehydrogenation, the extent of which fell far short of that needed to give the mass of the desired PAH **8** at 5760 Da.[17] For the cyclodehydrogenation of alkyl substituted HBCs,[4] the method of choice is to use iron(III) chloride, both Lewis acid and oxidizing agent in one. By predissolving the iron(III)

(13) Dilthey, W.; Hurtig, G. *Ber. Dtsch. Chem. Ges.* **1934**, *67*, 2004−2007.
(14) Wiesler, U. M.; Berresheim, A. J.; Morgenroth, F.; Lieser, G.; Müllen, K. *Macromolecules* **2001**, *34*, 187−199.
(15) Liu, D. J.; Zhang, H.; Grim, P. C. M.; De Feyter, S.; Wiesler, U. M.; Berresheim, A. J.; Müllen, K.; De Schryver, F. C. *Langmuir* **2002**, *18*, 2385−2391.
(16) Wind, M.; Wiesler, U. M.; Saalwächter, K.; Müllen, K.; Spiess, H. W. *Adv. Mater.* **2001**, *13*, 752−756.
(17) Przybilla, L.; Brand, J. D.; Yoshimura, K.; Räder, H. J.; Müllen, K. *Anal. Chem.* **2000**, *72*, 4591−4597.
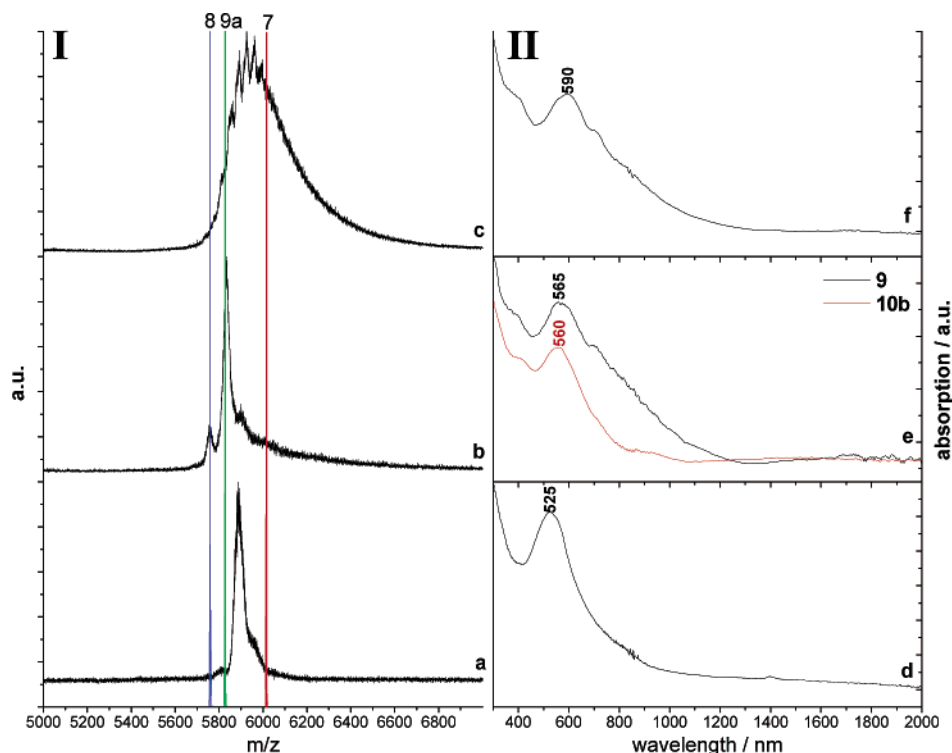
Figure 2. (I) MALDI-TOF mass spectra of cyclodehydrogenation products of dendrimer **7** (expanded region): (a) Experiment 1, 0.75 equiv of FeCl₃/H, 0.5 h; (b) Experiment 2, 1.5 equiv of FeCl₃/H, 20 h; (c) Experiment 3, 3.0 equiv of FeCl₃/H, 20 h. Yield (typically): ∼70−80%. The vertical lines represent the calculated masses of molecules **7**, **8**, and **9a**. (II) UV/vis spectra of thin films on quartz substrates corresponding to Experiments 1−3. In (e), the spectrum of model compound **10b** is also shown.

chloride in nitromethane, it can be added homogeneously to the solution of the dendrimer in methylene chloride.

One of the most crucial factors in the planarization reaction is the stoichiometry of cyclodehydrogenation reagent employed. Introduction of 0.75 equiv of iron(III) chloride per hydrogen to be removed results in a partially cyclized product with a peak maximum at 5890 Da (Figure 2a). The optimum amount for cyclodehydrogenation in this case turned out to be 1.5 equivalents, especially when employed in a 1:1 solvent mixture of methylene chloride and carbon disulfide as in Experiment 2 (Figure 2b). These conditions reproducibly result in a comparatively sharp main peak at 5830 Da, corresponding to the removal of about 200 hydrogens. A small peak at 5900 Da can be assigned to a 2-fold chlorination of this product, and a further small peak at 5760 Da indicated the formation of the fully planarized C474 disk **8**. Due to the different desorption behaviors of fully planarized disk and partially cyclized products, an exact quantification of the product distribution by mass spectrometry is not possible. Attempts to push the reaction further toward the completely planarized disk by employing up to 3−6 equiv of iron(III) chloride result only in higher molecular weight products with broader distribution, due to chlorination (Figure 2c). We see only minor differences between reactions quenched after 1 and 20 h.

While the insolubility of large PAHs severely limits classical solution characterization, solid-state methods are revealing. UV/vis spectra recorded after smearing a thin film of a sample from Experiment 2 on a quartz substrate show a surprisingly well-defined band at 565 nm (Figure 2e), sharper than that for a C222-PAH, which exhibits a very broad band at around 770 nm.[6] The obtained spectrum corresponded to a relatively defined PAH containing about 150 carbons, not to a C474 molecule in

which 200 hydrogens were randomly removed, where a broader and more bathochromically shifted band would be expected. This follows from a comparison with UV/vis spectra of other large PAHs with 42−222 carbons.[4,6]

We therefore propose that cyclodehydrogenation takes place independently in the three different arms of the dendrimer as suggested by the conformation of the dendritic precursor **7** (Figure 3a), leading to a partitioning and thus creating three large PAH subunits connected in the center with a 1,3,5-triphenylbenzene (**9a**) or benzene (**9b**) core. Such a molecule is propeller-shaped due to the steric hindrance of the "propeller blades" and conveniently explains why the cyclodehydrogenation is not proceeding further to the fully planarized disk **8**: the remaining hydrogens are simply too far apart to participate in a new carbon−carbon bond formation (Figure 3b,c). The close distance and favorable geometric arrangement of two carbon atoms are decisive for the bond closure, which also explains why there are no intermolecular reactions taking place. Thus, the cyclodehydrogenation is probably mainly progressing from the "outside" periphery toward the "inside" of the dendrimer. The aromatic "blades" of these propeller structures contain 150 and 156 carbons, respectively. The existence of these moieties satisfactorily explains the observed UV/vis and also the mass spectrum.

Part of the problem of exactly determining the composition and structure of the extremely large and insoluble cyclodehydrogenation product is the lack of isotopic resolution of the mass spectra. In principle, it is possible to obtain isotopic resolution in the investigated mass range with the used MALDI-TOF mass spectrometer (e.g., PMMA 6.000 Da standard or the dendrimer **7**). Due to the laser excitation wavelength of 337 nm and the UV/vis absorption of the investigated product, ionization does
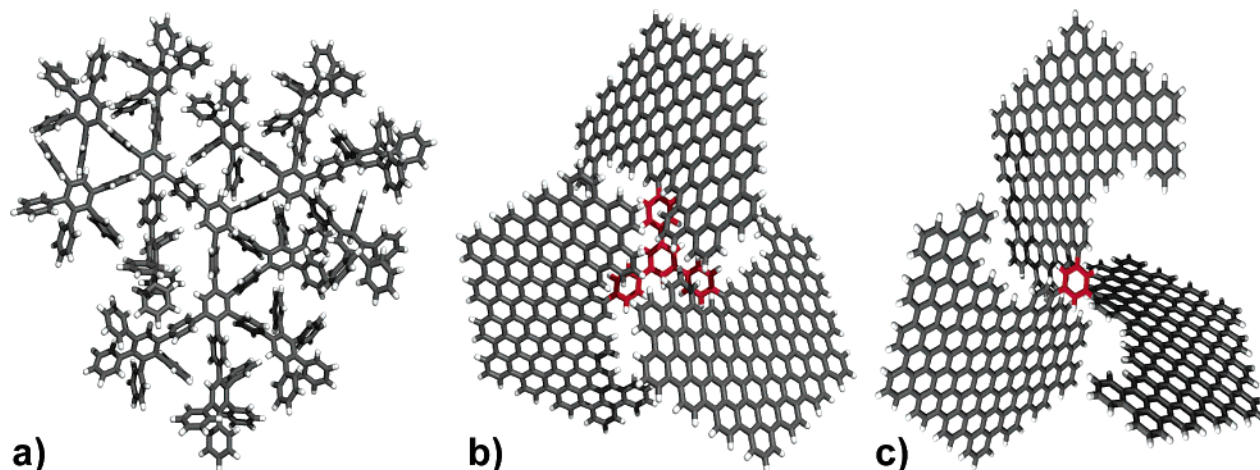
Figure 3. Computer-generated three-dimensional structures of (a) dendrimer **7**, (b) propeller with triphenylbenzene core **9a**, and (c) propeller with benzene core **9b**.[20]

Scheme 5. Synthesis of Model Compound **10b**[a]
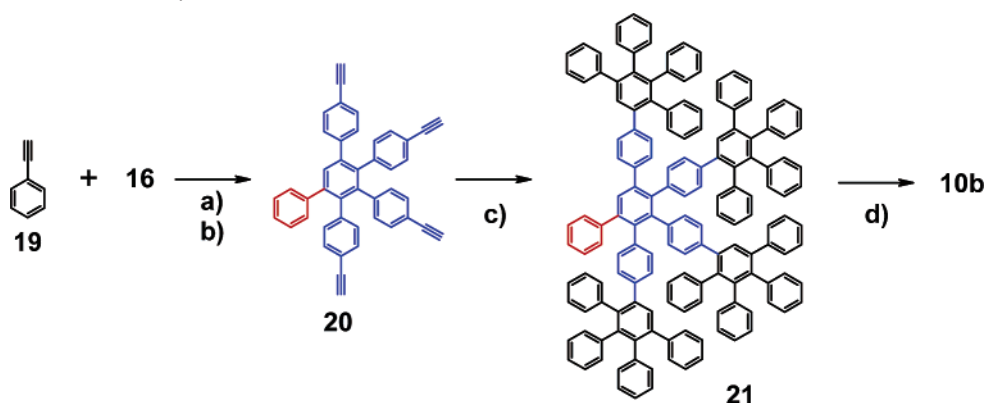
[a] Reagents, conditions, and yields: (a) *o*-xylene, 175 °C, 2 h, 98%; (b) NH₄F/Bu₄NF, THF, 10 min, 98%; (c) *o*-xylene, 175 °C, 14 h, 81%; (d) 3 equiv of AlCl₃/Cu(OTf)₂/H, CS₂, 24 h, 95%.

not take place by a conventional MALDI mechanism but by photoionization, leading to radical cations. We assume that the lack of high resolution is due to the higher internal energy of such molecules because of partial laser excitation, which, combined with the required high desorption energy, causes a peak broadening.

A possible solution to this problem was to chemically fragment the propeller molecule and to analyze the lower molecular weight fragments, which should be in the range of one-third of the original mass if the assumed structure above was true. Therefore, the cyclodehydrogenated product from Experiment 2 was heated for 30 min at 450 °C in an aluminum(III) chloride/sodium chloride melt, harsh conditions under which single aryl—aryl bonds are expected to break, while fused PAH segments should remain stable. Indeed, the resulting mass spectrum showed peaks at 1842 and 1914 Da, corresponding to the molecules **10a** and **10b.** At six mass units higher from each peak, there were additional peaks, obviously corresponding to defect structures with roughly three carbon—carbon bonds unclosed. This result indicates strongly that the 150 and 156 carbon-containing PAHs are present as subunits in the original molecule before fragmentation, therefore clearly proving the proposed partitioning of the cyclodehydrogenated molecule.

For a better comparison of the electronic properties of the propeller molecule, the C156 model compound **10b** was prepared in a separate approach (Scheme 5). The cyclopenta-

dienone **16** was reacted with an excess of phenylacetylene in a Diels—Alder cycloaddition until the purple color of **16** had disappeared. After subsequent cleavage of the silyl protective groups, the tetraacetylene compound **20** was obtained in 98% yield. A further [2+4] cycloaddition with **18** afforded the dendrimer **21**, which was cyclodehydrogenated to the 156-carbon PAH **10b**.

The solid-state UV/vis spectra of **9** and the model compound **10b** show a high degree of agreement, with **10b** also having a peak maximum at about 560 nm (Figure 2e). This indicates that both compounds contain the same or a very similar number of fused benzene rings within their conjugated system. The cyclodehydrogenation product **9** possesses an altogether broader spectrum and an additional shoulder, the cause of which is not quite clear. As expected, the partially closed product resulting from 0.75 equiv FeCl₃ has an absorption maximum at shorter wavelength (525 nm, Figure 2d), and the chlorinated product from Experiment 3 (3 equiv of FeCl₃, Figure 2f) has a bathochromic shifted maximum at 590 nm. It does seem possible to close even more bonds with higher equivalents, but the chlorinating side-reactions prevail.

Complementary to UV/vis spectroscopy, solid-state Raman spectroscopy is a further tool for the characterization of insoluble PAHs.[18] The profile of the Raman spectrum of **9**, characterized by two strong bands at 1603 and 1320 cm⁻¹, is very similar to that of **10b** (Figure 4). These two bands, usually referred to as
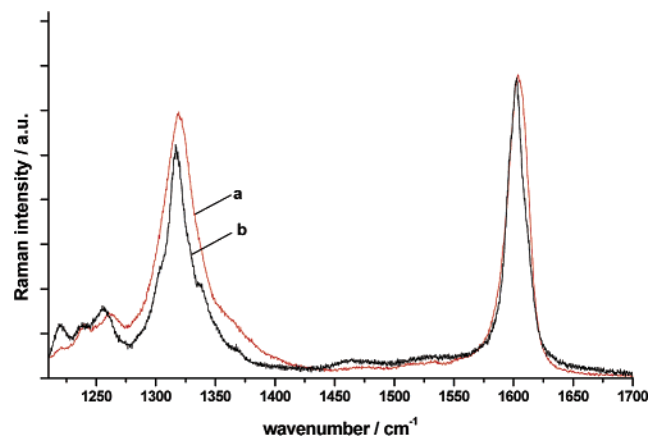
Figure 4. Raman spectra of propeller **9** (a) and the model compound **10b** (b).

the G- and D-bands, respectively, are typical features of PAHs, carbonaceous materials, and disordered graphite.[19] Slight differences between the two spectra (i.e., relative intensities and positions of the bands) appear in the spectral region at around 1300 cm^{-1} because of the higher sensitivity of the D-peak frequency to molecular size and geometry than the G-peak. Usually D-bands of PAHs show structured features composed of a very strong band and a few low intensity lines. Minor differences are observed in the positions of these low intensity peaks of the two compounds. The direct comparison of the two spectra also shows an increased intensity and broadening of the D-peak of **9** in relation to the D-peak of the model compound **10b**. For PAHs generally, the intensity of the D-peak with respect to the G-band is dependent on the degree of π-electron delocalization. The broadening of this band corresponds to the convolution of Raman transitions from a distribution of aromatic "domains" with different structures and dimensions. Therefore, two conclusions can be drawn from the Raman measurements: the subunits of the C474-propeller **9** and the C156 model compound **10b** are generally very similar; there are, however, some defect structures present in the "propeller blades".

A propeller-shaped model compound in which the partitioned aromatic domains were unambiguous should further assist in understanding the analytical data obtained for the propeller **9**. A suitable molecule can be prepared starting also from 1,3,5-tris-(4-iodophenyl)-benzene (**14**). By coupling **14** under Hagihara–Sonogashira conditions with a phenylacetylene and subsequent Diels–Alder reaction, an oligophenylene (**25**) is accessible, bearing three separate hexaphenylbenzene moieties, which cannot further interconnect. These can in turn be planarized individually by cyclodehydrogenation, so that a trimer of HBC-units (**26**) is formed, which is tethered in the center via a trigonal benzene connector (Scheme 6). To enable characterization by solution-based methods, alkyl substitution in the form of 3,7-dimethyloctyl chains was possible by employing suitably derivatized building blocks. Using 3 equiv of iron(III) chloride as reagent, **26** was successfully formed as a monodisperse compound by removing 36 hydrogens. According to the isotopically resolved MALDI-TOF mass spectrum,

(18) Shifrina, Z. B.; Averina, M. S.; Rusanov, A. L.; Wagner, M.; Müllen, K. *Macromolecules* **2000**, *33*, 3525–3529.
(19) Negri, F.; Castiglioni, C.; Tommasini, M.; Zerbi, G. *J. Phys. Chem. A* **2002**, *106*, 3306–3317.
(20) Using the molecular mechanics force field of Wavefunction Spartan Pro 1.0.5.

chlorination or partial cyclization defects could be avoided (Figure 5). The yellow compound was soluble under gentle warming in organic solvents such as chloroform, THF, and toluene. Solution NMR studies, however, resulted, even under heating, only in broad, unresolved spectra.

Due to the steric repulsion of the alkyl chain substituents, the trimer molecule is very unlikely to assume a planar conformation. The twisting of the three HBC-moieties out of plane leads to the formation of a propeller-shaped object, as illustrated by the calculated 3D-visualization in Figure 7. The three blades can be expected to possess a certain degree of rotational freedom around the bond connecting the core, thus explaining the good observed solubility. Excluding the flexible alkyl chains, such a rotor possesses a diameter of about 3 nm.

The out-of-plane twist of the HBC-sections is also confirmed by the absorption spectrum of the propeller molecule, which is depicted in Figure 6. The positions of the main bands are almost unchanged as compared to the hexaalkyl HBC-"monomer" **4a**. This proves that the aromatic chromophores in **26** are HBC-units, which are not in conjugation with each other. This is a result of the torsion angle with respect to the benzene linker and prevents an efficient electronic communication by overlap of the p$_z$ orbitals. The peak width of the bands of **26** is, however, increased. The comparison of the absorption spectra of the HBC-"monomer" and its propeller-shaped trimer bears a striking resemblance to the situation of the model compound C156 and the C474 propeller as seen in Figure 2e. This serves as a confirmation that an aromatic chromophore that is the same as or very similar to that of C156 is present in the C474 propeller.

Having clearly reached the limits of synthesis and spectroscopical characterization, it was desirable to further characterize the C474 propeller objects also by visualization, for example, by TEM. This attempt failed essentially because it was not possible to prepare separated single molecules from the insoluble compound on TEM grids. Only large particles with a very low degree of order down to about 100 nm were observed, corresponding to large clusters of the molecule.
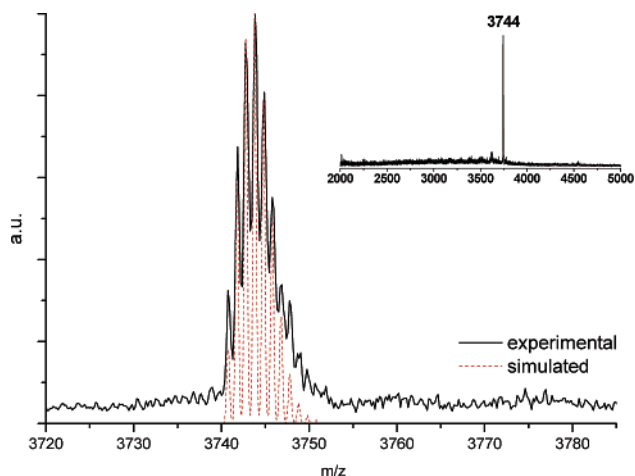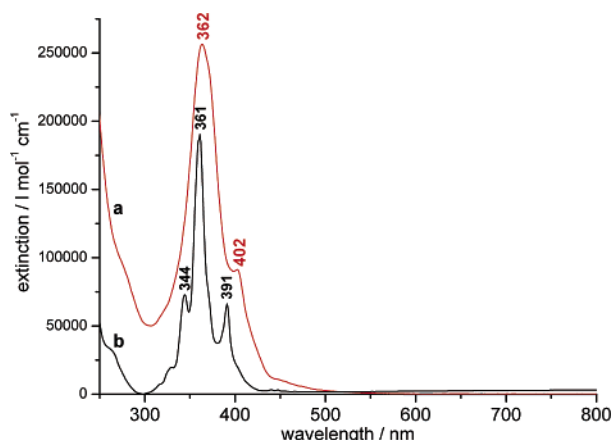
Nevertheless, the available spectroscopical structure analysis data were sufficient to be confident of the proposed three-dimensional structure of **9** and to move on to apply the cyclodehydrogenation conditions to a different geometric dendrimer structure.

The dendrimer **11** possesses a tetraphenylmethane core forcing the oligophenylene branches to adopt a tetrahedral geometry (Scheme 3 and Figure 8a) which thus prevents a complete planarization. Ideally, the removal of 136 hydrogens should afford four planarized wings consisting of rigid PAHs, which originate from the central core and point to the four corners of a tetrahedron. The resulting molecule resembles a tetra-bladed propeller (Figure 8c). The conditions for the oxidative cyclodehydrogenation of dendrimer **11** with iron(III) chloride were similar to those applied to the dendrimer **7**. A detailed analysis of the mass spectra became possible because isotopic resolution of the individual peaks could be achieved in this mass region. Using 0.75 equiv of iron(III) chloride per intendedly removed hydrogen led to a partially cyclodehydrogenated product with a peak maximum at 4800 Da. Employing 1.5 equiv afforded a product with the main peak at 4760 Da, much closer to the desired mass of 4749 Da for the target molecule **12c** (Figure 9). Even better results were obtained with

Scheme 6. Synthesis of HBC-Trimer **26**[a]
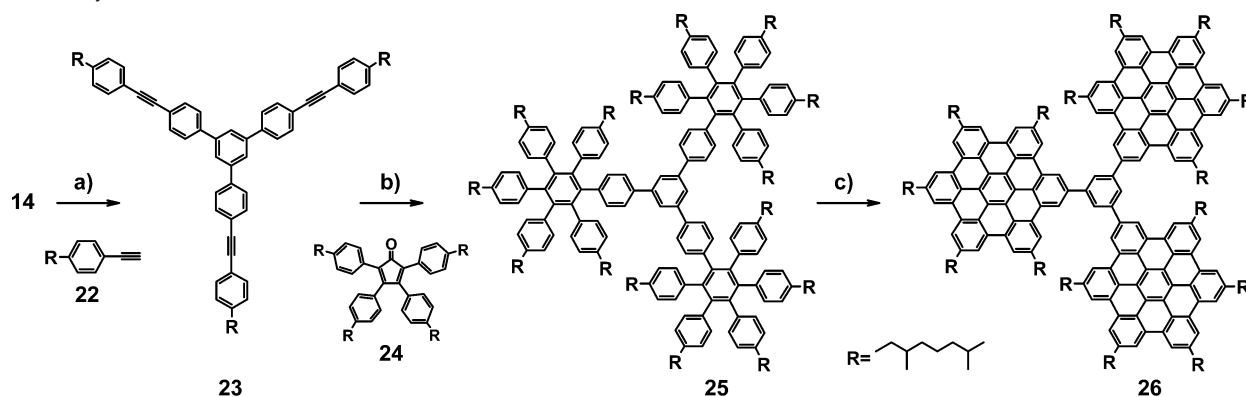
[a] Reagents, conditions, and yields: (a) CuI, Pd[PPh₃]₂Cl₂, PPh₃, NEt₃/THF (1:1), 83%; (b) Ph₂O, 260 °C, 3 d, 76%; (c) 3 equiv of FeCl₃/H, CH₃NO₂, CH₂Cl₂, 71%.


Figure 5. MALDI-TOF mass spectrum of the HBC-trimer **26**.

Figure 6. UV/vis spectra of chloroform solutions of (a) the HBC-trimer **26** and (b) the "monomer": HBC-(*n*-dodecyl)₆ (**4a**).

2−3 equiv of iron(III) chloride. In the case of 2.5 equiv, there is a weak chlorination peak at 4787 Da; however, the main product distribution is narrower than before, but still covers different degrees of cyclodehydrogenation. The optimum conditions were reached when 3 equiv was used, resulting in an even sharper main peak at 4753 Da. This peak corresponds to the removal of about 132 hydrogens from the precursor and supports the desired structure, however, with two carbon−carbon bonds missing to complete cyclodehydrogenation. A small peak at 4787 Da indicates monochlorination of this product.
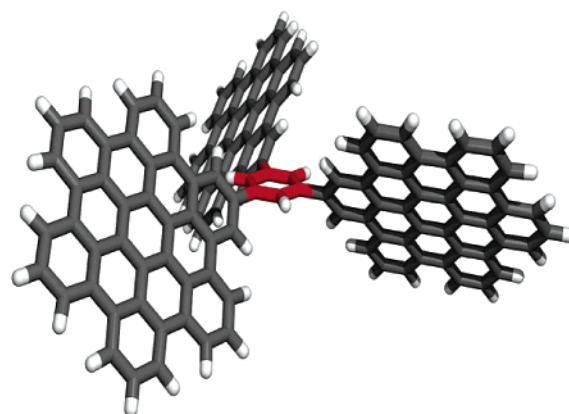

Figure 7. Computer-generated three-dimensional structure of the HBC-trimer **26** (alkyl chains omitted for clarity).[20]

With the assumption of a similar behavior in desorption and ionization for all products, the molecular weight distribution ascertains an average degree of cyclodehydrogenation of 96%. The total peak distribution covers the range from about 90% to 100% cyclodehydrogenation. The signal distribution within the MALDI-TOF mass spectrum can therefore be mainly attributed to a mixture of cyclodehydrogenation products covering the molecular formulas $C_{385}H_{124}$ to $C_{385}H_{134}$. The highest signal intensity can be found for compound $C_{385}H_{128}$ (**12b**), which is the most dominant species in the mixture. More drastic conditions to force the reaction to complete the removal of all hydrogens, however, favored the formation of higher molecular weight products attributable to chlorination. The spectrum resulting from the use of 6 equiv of iron(III) chloride contains further peaks assignable to products ranging from monochlorinated up to 6-fold chlorinated compounds in addition to the main signal at 4753 Da.

To further characterize the insoluble cyclodehydrogenated products **12**, they were also studied by solid-state spectroscopy. The UV/vis spectra of the "smeared" thin films of the samples showed, dependent on the quantities of iron(III) chloride, an absorption maximum successively red-shifted from 466 to 482 nm, correlated to the increasing size of the aromatic systems (Figure 10). The optical absorptions of the cyclodehydrogenated products using 2−3 equiv are very similar, and the well-defined band at 482 nm is comparable to that observed for a PAH with 96 carbon atoms ($C_{96}H_{30}$).[4] This resemblance indicates that the investigated molecules are composed of four separate wings
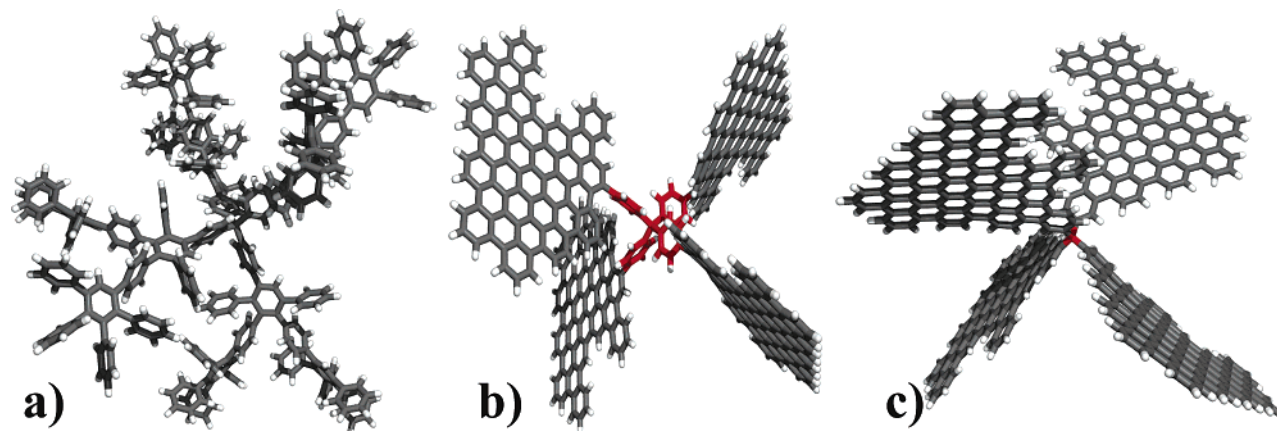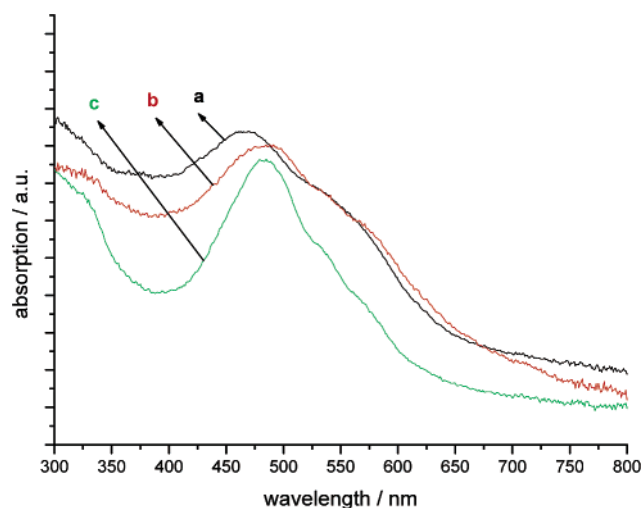
Figure 8. Computer-generated three-dimensional structures of (a) dendrimer **11** (b) propeller with tetraphenylmethane core **12a**, and (c) fully cyclized propeller **12c**.[20]
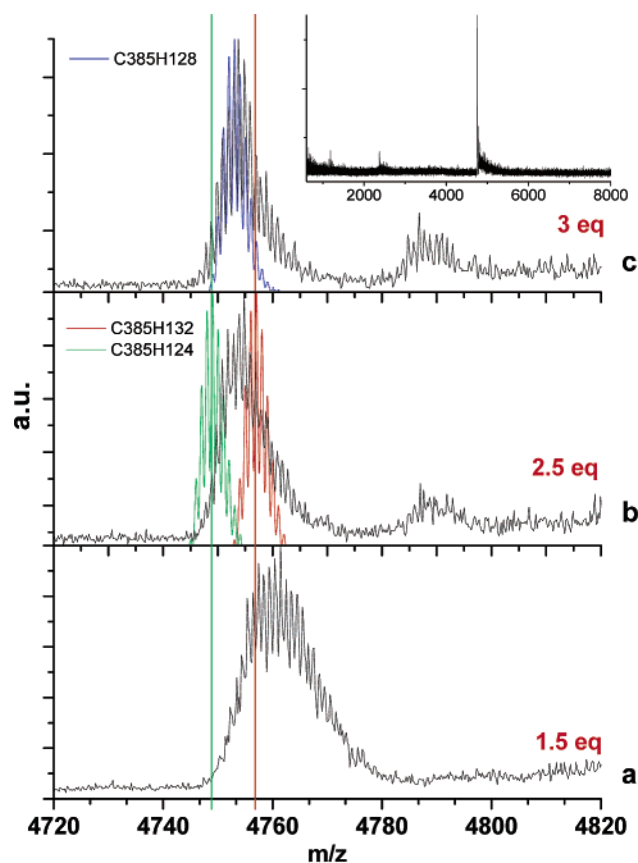

Figure 9. MALDI-TOF mass spectra of cyclodehydrogenation products of dendrimer **11** (expanded region): (a) 1.5 equiv of $FeCl_3$/H, 20 h; (b) 2.5 equiv of $FeCl_3$/H, 20 h; (c) 3.0 equiv of $FeCl_3$/H, 20 h. Yield (typically): ∼80−90%. The vertical lines represent the calculated masses of molecules **12a** and **12c**. The colored graphs (red, blue, and green) represent the simulated mass spectra for **12a**, **12b**, and **12c**, respectively. Inset: Full range of spectrum c.


Figure 10. UV/vis spectra of the cyclodehydrogenation products of dendrimer **11** using (a) 0.75 equiv of $FeCl_3$/H; (b) 1.5 equiv of $FeCl_3$/H; (c) 2.5 equiv of $FeCl_3$/H.
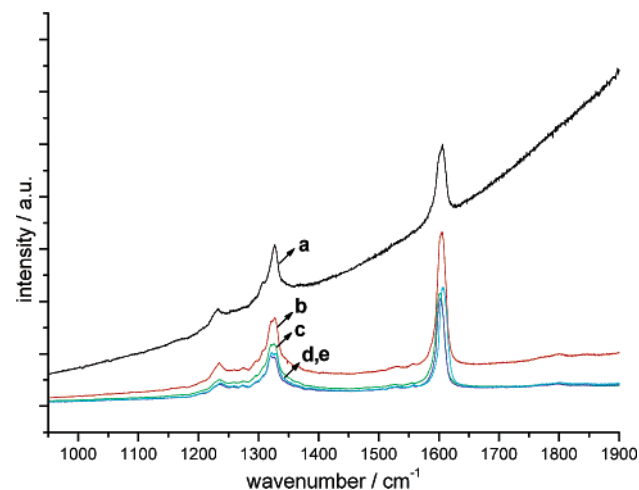
Figure 11. Raman spectra of the cyclodehydrogenation products of dendrimer **11** using (a) 0.75 equiv of $FeCl_3$/H; (b) 1.5 equiv of $FeCl_3$/H; (c) 2.0 equiv of $FeCl_3$/H; (d) 2.5 equiv of $FeCl_3$/H; (e) 3.0 equiv of $FeCl_3$/H (λ_{ex} = 514.5 nm).

consisting of conjugated systems with approximately 96 carbons each.

By applying Raman spectroscopy, relevant information about the degree of cyclodehydrogenation in relation to the number of employed iron(III) chloride equivalents could be obtained. All of the solid-state Raman spectra showed, with minor differences, as common features a first strong band located at 1324 cm^{-1}, a weak band at 1234 cm^{-1}, and a second strong band located at 1602 cm^{-1} (Figure 11). A significant difference

of these spectra is their decreasing background intensity, with increasing number of equivalents of iron(III) chloride used for cyclodehydrogenation. This behavior can be attributed to a fluorescence effect. The fluorescence appears as a broad spectral
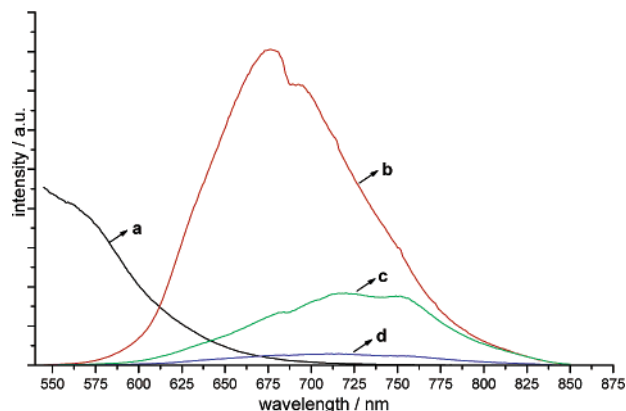
Figure 12. Solid-state fluorescence spectra of dendrimer **11** (a) and of its cyclodehydrogenation products using (b) 0.75 equiv of $FeCl_3/H$; (c) 1.5 equiv of $FeCl_3/H$; (d) 2.5 equiv of $FeCl_3/H$ ($\lambda_{ex} = 514.5$ nm).

emission which adds to the background and is an indication of the amount of partially cyclized structures in the product.

This finding is supported by the solid-state emission spectrum of the cyclodehydrogenated propeller structures. Using 0.75 equiv for cyclodehydrogenation, the fluorescence is very intense (Figure 12). Upon the addition of higher iron(III) chloride equivalents, there is a distinct decrease in fluorescence intensity, as well as a shift of the emission spectrum to longer wavelengths. As in the Raman spectra, this decrease can also be correlated to an increase of the degree of cyclization in the propeller molecule.

These solid-state spectroscopical results serve as complementary confirmations of the results already obtained by mass spectrometry. They are of particular interest as independent sources of information concerning the degree of cyclodehydrogenation for other insoluble, for example, polymeric, carbon-rich compounds where mass spectrometry is no longer an option.

Conclusions

It has been demonstrated that the concept of completely planarizing large oligophenylenes reaches its limit when the dendrimer becomes so big that the cyclodehydrogenation reaction takes place preferentially within the dendritic arms and not in between. This partitioning results, however, in a new approach to propeller-like, three-dimensional molecular structures with large PAH subunits. As originally expected, the cyclodehydrogenation reaction for such a giant molecule cannot be 100% efficient. While the cyclodehydrogenation still yields a monodisperse product for the HBC-trimer **26**, with the increased number of individual bond formation steps as in the reaction of the larger, second-generation dendrimers **7** and **11**, some degree of defects have to be taken into account. As

indicated by various analysis methods, these imperfections consist of a few unclosed bonds in the PAH "wings" and a small content of chlorination. The defects, however, have no effect on the basic propeller structure of the molecules and the significant findings of this study. Even without an exact quantification of the product distribution, the individual bond formation of the oxidative cyclodehydrogenation reaction can be considered to have an extremely high efficiency, which is impressive taking into account the large size and unfavorable solubility properties of the studied compounds. The optimal stoichiometry, that is, the number of equivalents of cyclodehydrogenation reagent, is, however, very dependent on the individual molecule and can vary considerably.

We succeeded in the synthesis of new nanometer scale structures consisting of three and four PAH wings tethered by a central core, with diameters ranging from about 3 to 4.5 nm. The combination of spectroscopic and spectrometric methods used for their structure elucidation proved highly revealing in cases where no single technique could provide clear answers anymore.

While on the single molecule side the appealing propeller shape is of great interest, the torsion of the PAH-"blades" with respect to each other also must have implications on the bulk state of the molecule. It can be expected that the graphene-like subunits of different molecules are not arranged in large coplanar domains as in graphite itself, but rather in small microdomains tilted at different angles. The exact nature of this packing behavior, however, remains to be studied more closely.

Further investigations toward the visualization, manipulation, and application in hydrogen storage of these new 3D nanopropellers are underway. Also, there is sufficient ground to believe that introduction of alkyl chain substituents on the periphery will make these large structures soluble and thus processable.

Supporting Information Available: Full experimental and spectroscopic information of the presented compounds (PDF). This material is available free of charge via the Internet at http://pubs.acs.org.

JA036732J